

Search for anomalous quartic $\gamma\gamma WW$ couplings in dielectron and missing energy final states with 9.7 fb^{-1} in $p\bar{p}$ collisions at $\sqrt{s} = 1.96 \text{ TeV}$ - D0

Émilien Chapon, on behalf of the D0 collaboration*

SPP / Irfu / CEA Saclay

E-mail: emilien.chapon@cern.ch

We present the search for anomalous quartic gauge boson couplings ($\gamma\gamma WW$) from the study of events with two opposite charge electrons and missing transverse energy. The analyzed data correspond to 9.7 fb^{-1} of integrated luminosity collected by the D0 detector in $p\bar{p}$ collisions at $\sqrt{s} = 1.96 \text{ TeV}$. The presence of anomalous quartic gauge couplings would manifest itself as an excess of very boosted WW events. No such excess is found in the data and we improve on the best published limits at the time of the communication on the anomalous parameters a_0^W and a_C^W .

PACS: 14.70.Fm, 12.60.Cn, 13.85.Qk

*International Conference on the Structure and the Interactions of the Photon including the 20th International Workshop on Photon-Photon Collisions and the International Workshop on High Energy Photon Linear Colliders
20 - 24 May 2013
Paris, France*

*Speaker.

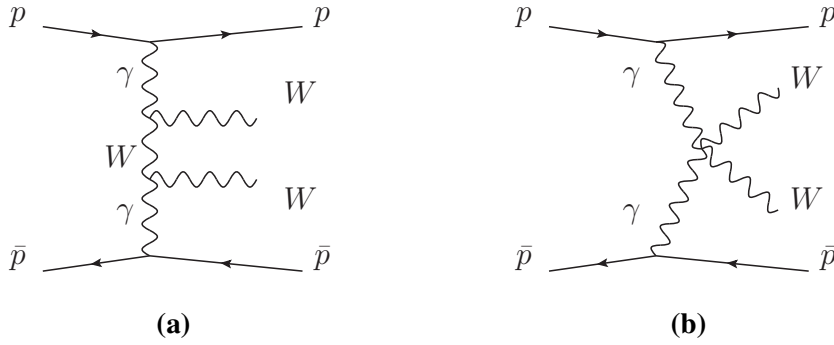


Figure 1: Diagrams contributing to W boson pair production via photon exchange, with (a) triple $WW\gamma$ and (b) quartic $WW\gamma\gamma$ couplings.

1. Theoretical framework

We study the exclusive W boson pair production through photon exchange in proton-antiproton collisions. The cross section for this process is very small in the standard model of particle physics (SM), $\sigma_{p\bar{p}\rightarrow p\bar{p}WW} \approx 3$ fb. However it is sensitive to beyond standard model effects, especially anomalous quartic gauge boson couplings (AQGCs) [1]. The two leading-order diagrams contributing to this process are shown on Figure 1. In this analysis, we only study AQGCs, while the triple gauge boson couplings (TGCs) are assumed to be at their SM values.

The parameterization of the AQGCs is based on Ref. [2] and only the lowest dimension operators that have the correct Lorentz invariant structure and fulfill $SU(2)_C$ custodial symmetry [3] are considered. Such operators involving two W bosons and two photons final state are of dimension six:

$$\begin{aligned}\mathcal{L}_6^0 &= \frac{-e^2}{8} \frac{a_0^W}{\Lambda^2} F_{\mu\nu} F^{\mu\nu} W^{+\alpha} W_{\alpha}^- \\ \mathcal{L}_6^C &= \frac{-e^2}{16} \frac{a_C^W}{\Lambda^2} F_{\mu\alpha} F^{\mu\beta} (W^{+\alpha} W_{\beta}^- + W^{-\alpha} W_{\beta}^+),\end{aligned}\quad (1.1)$$

where $F^{\mu\nu}$ is the electromagnetic field strength tensor and W_{α}^{\pm} is the W^{\pm} boson field. a_0^W and a_C^W are the usual notation for the parametrized quartic coupling constants, where a non-zero a_0^W could be due to an exchange of a heavy neutral scalar, while heavy charged fermions would contribute to both a_0^W and a_C^W . The new scale Λ is introduced so that the Lagrangian density has the correct dimension of four and is interpreted as the typical mass scale of new physics.

The $p\bar{p} \rightarrow p\bar{p}W^+W^-$ cross section via photon exchange rises quickly at high energies when the anomalous coupling parameters are non-zero and manifests itself in particular with the production of boosted W boson pairs. In the SM, the $\gamma\gamma \rightarrow WW$ cross section is constant in the high-energy limit due to the cancellation between the relevant diagrams. When the new quartic terms are added, the cancellation does not hold and the cross section will grow to violate unitarity at high energies. This increase of the cross section can be regularized with a form factor that reduces the values of a_0^W and a_C^W at high energy while not modifying them at lower energies. Following a standard

approach, we introduce the following form factor [4]:

$$a_i^W \rightarrow \frac{a_i^W}{(1 + M_{\gamma\gamma}^2/\Lambda_{\text{cutoff}}^2)^2}, \quad (1.2)$$

where $M_{\gamma\gamma}$ is the invariant mass of the two photons and Λ_{cutoff} is chosen to be either 0.5 or 1 TeV, following the prescription of, e.g., Ref. [4]. In the following, we provide limits on anomalous couplings with and without form factors.

The best 95% C.L. published limits on these anomalous parameters at the time of the communication came from the OPAL Collaboration from measurement of $WW\gamma$, $q\bar{q}\gamma\gamma$, and $\nu\bar{\nu}\gamma\gamma$ production [5] at the CERN LEP Collider:

$$\begin{aligned} -0.020 \text{ GeV}^{-2} &< a_0^W/\Lambda^2 < 0.020 \text{ GeV}^{-2} \\ -0.052 \text{ GeV}^{-2} &< a_C^W/\Lambda^2 < 0.037 \text{ GeV}^{-2}. \end{aligned} \quad (1.3)$$

These constraints were recently superseded by a new result from the CMS Collaboration at the LHC Collider [6]:

$$\begin{aligned} |a_0^W/\Lambda^2| &< 0.00015 \text{ GeV}^{-2} \quad (a_C^W/\Lambda^2 = 0, \Lambda_{\text{cutoff}} = 500 \text{ GeV}) \\ |a_C^W/\Lambda^2| &< 0.0005 \text{ GeV}^{-2} \quad (a_0^W/\Lambda^2 = 0, \Lambda_{\text{cutoff}} = 500 \text{ GeV}). \end{aligned} \quad (1.4)$$

2. Data and Monte-Carlo samples

The full Run II set of data recorded by the D0 detector is considered in this analysis [7], representing 9.7 fb^{-1} of $p\bar{p}$ collisions at $\sqrt{s} = 1.96 \text{ TeV}$ delivered by the Tevatron between 2002 and 2011, after the relevant data quality requirements are invoked. The innermost part of the D0 detector is composed of a central tracking system with a silicon microstrip tracker (SMT) and a central fiber tracker inside a 2 T solenoidal magnet. The tracking system is surrounded by a central preshower detector and a liquid-argon/uranium calorimeter with electromagnetic, fine, and coarse hadronic sections. The central calorimeter (CC) covers pseudorapidity $|\eta_d| \lesssim 1.1$ [8]. Two end calorimeters (EC) extend the coverage to $1.4 \lesssim |\eta_d| \lesssim 4.2$. Energy sampling in the region between the ECs and CC is improved by the addition of scintillating tiles. A muon spectrometer, with pseudorapidity coverage of $|\eta_d| \lesssim 2$, resides outside the calorimetry and is comprised of drift tubes, scintillation counters, and toroidal magnets. Trigger decisions are based on information from the tracking detectors, calorimeters, and muon spectrometer. Details on the reconstruction and identification criteria for electrons, jets, and missing transverse energy, \cancel{E}_T , can be found elsewhere [9]. In this paper we call both electrons and positrons “electrons,” with the charge of the particle determined from the curvature of the associated tracks in the central tracking system.

The bulk of the analysis presented here is common with the D0 search for the Higgs boson in the $H \rightarrow W^+W^- \rightarrow \ell^+\nu\ell^-\bar{\nu}$ channel that is described in detail elsewhere [9]. We are looking for

the final state with a pair of W bosons decaying to two opposite sign electrons and two neutrinos, leading to two high-momentum electrons and missing transverse energy. The $p\bar{p} \rightarrow W^+W^-$ cross section has been measured in the $H \rightarrow W^+W^-$ analysis; however, there are a few specificities to our search for AQGCs. Only the $e^+ve^-\bar{\nu}$ final state has been considered, and the search has been optimized, of course, for the AQGC signal instead of the Higgs boson signal.

The background where, like the signal, the proton and the antiproton are intact in the final state, originates from photon exchange and double pomeron exchange (DPE) processes [10]. Both these backgrounds and the AQGC signals are modeled using the FPMC [11] generator, followed by a detailed GEANT3-based [12] simulation of the D0 detector. Diffractive and photon exchange backgrounds to this search are exclusive e^+e^- and $\tau^+\tau^-$ production through t -channel photon exchange (Drell-Yan) and inclusive W^+W^- , e^+e^- , and $\tau^+\tau^-$ production through DPE.

Since the outgoing intact proton and antiproton are not detected in this measurement, we also need to consider non-diffractive backgrounds. These backgrounds are Z/γ^* +jets, $t\bar{t}$ and diboson (W^+W^- , $W^\pm Z$, and ZZ) production, and processes in which jets are misidentified as electrons: W +jets and multijet production. The simulated samples used to model them are identical to those described in Ref. [9]. All of these backgrounds, except multijet production, are modeled using the PYTHIA [13] or ALPGEN [14] generator, with PYTHIA providing showering and hadronization in the latter case, using the CTEQ6L1 [15] parton distribution functions (PDFs). The multijet background is determined from the data by inverting some electron selection criteria, as described in Ref. [9].

The signal cross section is very small in the SM, being $\sigma(p\bar{p} \rightarrow p\bar{p}W^+W^-) = 3$ fb. After event selection, we are left with 0.1 expected event in our data sample. However, we can expect a very large enhancement (by up to two orders of magnitude) in the presence of anomalous couplings.

3. Analysis techniques

We define two stages in our event selection. The first stage, called the preselection, requires two opposite-sign electrons, with a transverse momentum larger than 10 GeV (15 GeV for the leading electron). The electrons must be reconstructed in the CC ($|\eta_D| < 1.1$) or in the EC ($1.5 < |\eta_D| < 2.5$), with at least one electron required to be in the CC. The invariant mass of the two electrons must be higher than 15 GeV. At last, there must be no reconstructed jet in the event with a transverse momentum higher than 20 GeV.

The distribution of the leading electron p_T is shown on Figure 2 after the preselection. The background simulation models the data very well, and after the preselection non-diffractive Z/γ^* production is the dominant background. In the presence of AQGCs, we expect a boosted W boson pair from the signal. Similar effects are expected from a non-zero a_0^W or a_C^W .

The next step is to reject the dominant Z/γ^* background. Following the same strategy as in the $H \rightarrow W^+W^- \rightarrow \ell^+v\ell^-\bar{\nu}$ analysis, a Boosted Decision Tree (BDT) is used. A tight cut on the output of this BDT allows to reject most of the Z/γ^* background, but also of the multijet background, and of the photon exchange and DPE backgrounds. At the same time, this cut on the BDT output has a very high efficiency on our signal.

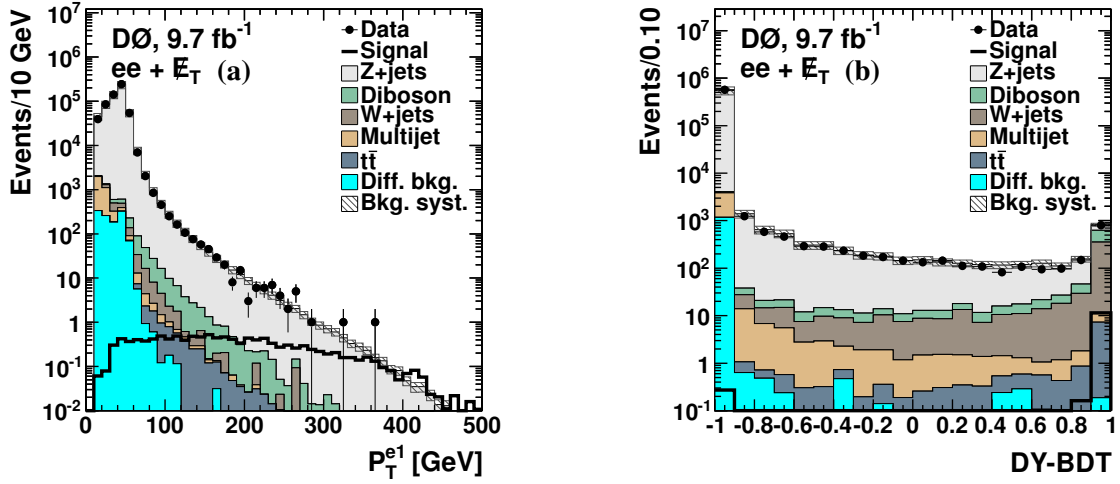


Figure 2: (a) Leading electron p_T at the preselection level and (b) output of the BDT used to reject the Z/γ^* background at the preselection level. The hatched bands show the total systematic uncertainty on the background prediction. The signal distributions are those expected for $a_0^W/\Lambda^2 = 5 \times 10^{-4} \text{ GeV}^{-2}$ and no form factor.

	Preselection	Final selection
Data	572700	946
Total background	576576 ± 11532	983 ± 108
Signal	12.2	11.6
$Z/\gamma^* \rightarrow ee$	566800	291
$Z/\gamma^* \rightarrow \tau\tau$	4726	22
$t\bar{t}$	15	8
W+jets	623	370
Diboson	517	287
Multijet	2716	5.4
Diff. bkg. (γ exch. and DPE)	1180	0.2

Table 1: Observed and expected numbers of events after the preselection and the final selection for data, signal ($a_0^W/\Lambda^2 = 5 \times 10^{-4} \text{ GeV}^{-2}$ and no form factor), and the different backgrounds considered in the analysis.

A final BDT is trained to separate the AQCW signal from all the other backgrounds. The same BDT is used in the study of both parameters a_0^W and a_C^W , which feature similar kinematic characteristics.

Systematic uncertainties are estimated for the signal and for each background process. They can affect only the normalization or both the normalization and the shape of the final discriminant.

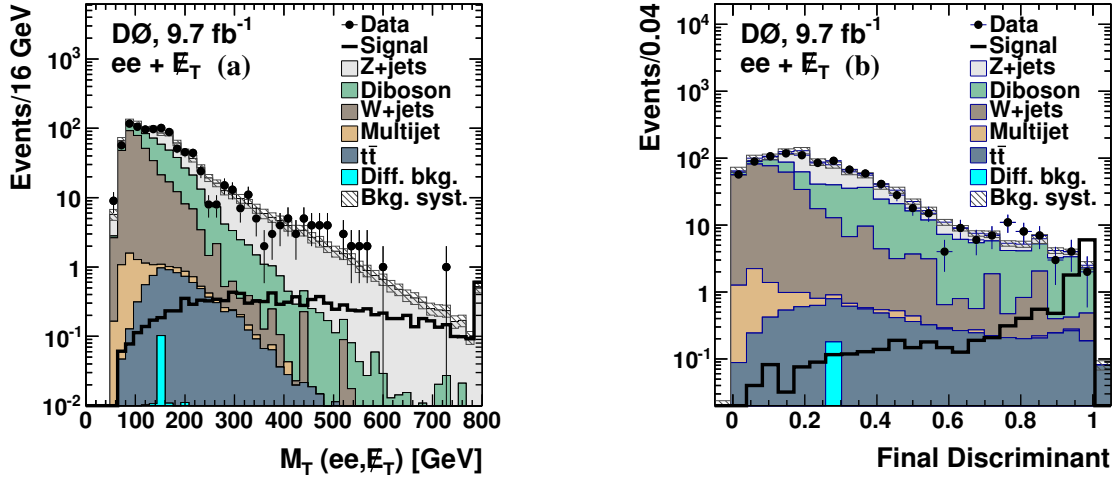


Figure 3: (a) Transverse mass of the \cancel{E}_T and the two electrons after the final selection and (b) output of the final BDT discriminant after the final selection. The hatched bands show the total systematic uncertainty on the background prediction. The signal distributions are those expected for $a_0^W/\Lambda^2 = 5 \times 10^{-4} \text{ GeV}^{-2}$ and no form factor.

Cutoff	Expected upper limit [GeV^{-2}]	Observed upper limit [GeV^{-2}]
No form factor	0.00043	0.00043
$\Lambda_{\text{cutoff}} = 1 \text{ TeV}$	0.00092	0.00089
$\Lambda_{\text{cutoff}} = 0.5 \text{ TeV}$	0.0025	0.0025

Table 2: Expected and observed 95% C.L. upper limits on $|a_0^W/\Lambda^2|$, assuming a_C^W is zero and for different assumptions about the form factor.

4. Results

The data are found to be in good agreement with the background-only prediction, and upper limits are set on the anomalous parameters a_0^W and a_C^W . The 95% C.L. allowed ranges for the anomalous parameter a_0^W (a_C^W) can be found in Table 2 (3), assuming a_C^W (a_0^W) is zero. The limits are quoted both without a form factor and for a form factor with $\Lambda_{\text{cutoff}} = 1$ or 0.5 TeV (as advised, e.g., in Ref. [4]). The two-parameter limits are shown in Fig. 4 for different assumptions about the signal, namely if no form factor is used and if a form factor is used with $\Lambda_{\text{cutoff}} = 1$ or 0.5 TeV. The two-parameter 68% C.L. (95% C.L.) limits define the range of values of the anomalous coupling parameters for which the theoretical cross section is lower than the upper 68% C.L. (95% C.L.) limit on the signal cross section, obtained in the single parameter limits.

5. Conclusion

We have presented a way to probe the electroweak sector of the SM using dielectron plus missing transverse energy final states, with new constraints on anomalous $WW\gamma\gamma$ quartic gauge boson

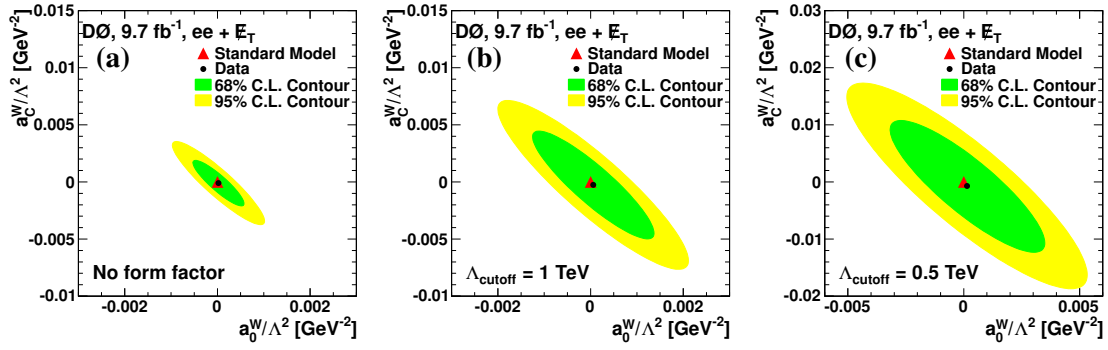


Figure 4: Two-parameter 68% and 95% C.L. limits with different assumptions about the signal: (a) no form factor, or a form factor with (b) $\Lambda_{\text{cutoff}} = 1$ or (c) 0.5 TeV.

Cutoff	Expected upper limit [GeV^{-2}]	Observed upper limit [GeV^{-2}]
No form factor	0.0016	0.0015
$\Lambda_{\text{cutoff}} = 1$ TeV	0.0033	0.0033
$\Lambda_{\text{cutoff}} = 0.5$ TeV	0.0090	0.0092

Table 3: Expected and observed 95% C.L. upper limits on $|a_c^W/\Lambda^2|$, assuming a_0^W is zero and for different assumptions about the form factor.

couplings. When a form factor with $\Lambda_{\text{cutoff}} = 0.5$ TeV is used, the observed upper limits at 95% C.L. on the anomalous parameters are $|a_0^W/\Lambda^2| < 0.0025 \text{ GeV}^{-2}$ and $|a_c^W/\Lambda^2| < 0.0092 \text{ GeV}^{-2}$. These are more stringent than the best published limits at the time of the conference and represent the only limits on AQGC from a Tevatron experiment.

6. Acknowledgements

We thank the staffs at Fermilab and collaborating institutions, and acknowledge support from the DOE and NSF (USA); CEA and CNRS/IN2P3 (France); MON, NRC KI and RFBR (Russia); CNPq, FAPERJ, FAPESP and FUNDUNESP (Brazil); DAE and DST (India); Colciencias (Colombia); CONACyT (Mexico); NRF (Korea); FOM (The Netherlands); STFC and the Royal Society (United Kingdom); MSMT and GACR (Czech Republic); BMBF and DFG (Germany); SFI (Ireland); The Swedish Research Council (Sweden); and CAS and CNSF (China).

References

- [1] E. Chapon, C. Royon and O. Kepka, *Anomalous quartic $WW\gamma\gamma$, $ZZ\gamma\gamma$, and trilinear $WW\gamma$ couplings in two-photon processes at high luminosity at the LHC*, *Phys. Rev. D* **81** (2010) 074003 [arXiv:0912.5161 [hep-ph]].
- [2] G. Belanger and F. Boudjema, *$\gamma\gamma \rightarrow W^+W^-$ and $\gamma\gamma \rightarrow ZZ$ as tests of novel quartic couplings*, *Phys. Lett. B* **288** (1992) 210. In the present study, the a_0^Z and a_c^Z parameters are assumed to be zero.

- [3] R. A. Diaz and R. Martinez, *The Custodial symmetry*, *Rev. Mex. Fis.* **47**, 489 (2001) [hep-ph/0302058].
- [4] O. J. P. Eboli, M. C. Gonzalez-Garcia, S. M. Lietti and S. F. Novaes, *Anomalous quartic gauge boson couplings at hadron colliders*, *Phys. Rev. D* **63**, 075008 (2001) [hep-ph/0009262].
- [5] G. Abbiendi *et al.* [OPAL Collaboration], *Constraints on anomalous quartic gauge boson couplings from $\nu\bar{\nu}\gamma\gamma$ and $q\bar{q}\gamma\gamma$ events at LEP-2*, *Phys. Rev. D* **70**, 032005 (2004) [hep-ex/0402021].
- [6] S. Chatrchyan *et al.* [CMS Collaboration], *Study of exclusive two-photon production of W^+W^- in pp collisions at $\sqrt{s} = 7$ TeV and constraints on anomalous quartic gauge couplings*, *JHEP* **1307** (2013) 116 [arXiv:1305.5596 [hep-ex]].
- [7] V. M. Abazov *et al.* [D0 Collaboration], *Search for anomalous quartic $WW\gamma\gamma$ couplings in dielectron and missing energy final states in $p\bar{p}$ collisions at $\sqrt{s} = 1.96$ TeV*, *Phys. Rev. D* **88** (2013) 012005 [arXiv:1305.1258 [hep-ex]].
- [8] The pseudorapidity is defined as $\eta = -\ln(\tan\theta/2)$, where θ is the polar angle relative to the proton beam direction. η_d is the detector pseudorapidity, calculated using the position of the calorimeter cluster with respect to the center of the detector.
- [9] V. M. Abazov *et al.* [D0 Collaboration], *Search for Higgs boson production in oppositely charged dilepton and missing energy final states in 9.7 fb^{-1} of $p\bar{p}$ collisions at $\sqrt{s} = 1.96$ TeV*, *Phys. Rev. D* **88** (2013) 052006 [arXiv:1301.1243 [hep-ex]].
- [10] M. Boonekamp, F. Chevallier, C. Royon, and L. Schoeffel, *Understanding the Structure of the Proton: From HERA and Tevatron to LHC*, *Acta Phys. Polon. B* **40**, 2239 (2009) [arXiv:0902.1678 [hep-ph]].
- [11] Forward Physics Monte Carlo (FPMC): M. Boonekamp, V. Juránek, O. Kepka, and C. Royon, in *Proceedings of the Workshop of the Implications of HERA for LHC Physics*, Hamburg-Geneva, 2006-2008, p. 758; M. Boonekamp *et al.*, [arXiv:1102.2531v1 [hep-ph]], <http://cern.ch/fPMC>.
- [12] R. Brun and F. Carminati, CERN Program Library Long Writeup W5013, 1993 (unpublished).
- [13] T. Sjostrand, S. Mrenna and P. Z. Skands, *PYTHIA 6.4 Physics and Manual*, *JHEP* **0605** (2006) 026 [hep-ph/0603175]; we use versions 6.319 and 6.413.
- [14] M. L. Mangano, M. Moretti, F. Piccinini, R. Pittau and A. D. Polosa, *ALPGEN, a generator for hard multiparton processes in hadronic collisions*, *JHEP* **0307** (2003) 001 [hep-ph/0206293]; we use version 2.11.
- [15] J. Pumplin, D. R. Stump, J. Huston, H. L. Lai, P. M. Nadolsky and W. K. Tung, *New generation of parton distributions with uncertainties from global QCD analysis*, *JHEP* **0207** (2002) 012 [hep-ph/0201195].